Experimental Brain Research (2019) 237:2983–2993
https://doi.org/10.1007/s00221-019-05644-6

RESEARCH ARTICLE

Pleiotrophin increases neurite length and number of spiral ganglion neurons in vitro

Sebastian Bertram[1] · Lars Roll[2] · Jacqueline Reinhard[2] · Katharina Groß[2] · Stefan Dazert[1] · Andreas Faissner[2] · Stefan Volkenstein[1]

Received: 1 April 2019 / Accepted: 3 September 2019 / Published online: 12 September 2019

Abstract

Acoustic trauma, aging, genetic defects or ototoxic drugs are causes for sensorineural hearing loss involving sensory hair cell death and secondary degeneration of spiral ganglion neurons. Auditory implants are the only available therapy for severe to profound sensorineural hearing loss when hearing aids do not provide a sufficient speech discrimination anymore. Neurotrophic factors represent potential therapeutic candidates to improve the performance of cochlear implants (CIs) by the support of spiral ganglion neurons (SGNs). Here, we investigated the effect of pleiotrophin (PTN), a well-described neurotrophic factor for different types of neurons that is expressed in the postnatal mouse cochlea. PTN knockout mice exhibit severe deficits in auditory brainstem responses, which indicates the importance of PTN in inner ear development and function and makes it a promising candidate to support SGNs. Using organotypic explants and dissociated SGN cultures, we investigated the influence of PTN on the number of neurons, neurite number and neurite length. PTN significantly increased the number and neurite length of dissociated SGNs. We further verified the expression of important PTN-associated receptors in the SG. mRNA of anaplastic lymphoma kinase, α_v integrin, β_3 integrin, receptor protein tyrosine phosphatase β/ζ, neuroglycan C, low-density lipoprotein receptor-related protein 1 and syndecan 3 was detected in the inner ear. These results suggest that PTN may be a novel candidate to improve sensorineural hearing loss treatment in the future.

Keywords Cochlea · Hearing loss · Neurite growth · Neurotrophin · Organotypic explant

Abbreviations

ALK	Anaplastic lymphoma kinase
BDNF	Brain-derived neurotrophic factor
BM	Basic medium
BMP-2	Bone morphogenetic protein-2
CI	Cochlear implant
DRG	Dorsal root ganglion
GDNF	Glial cell line-derived neurotrophic factor
HARP	Heparin affinity regulatory peptide
HB-GAM	Heparin-binding growth-associated molecule
HBBM	Heparin-binding brain mitogen
HBGF-8	Heparin-binding growth factor 8
HC	Hair cell
LIF	Leukemia inhibitory factor
LN	Laminin
LRP1	Low-density lipoprotein receptor-related protein
MK	Midkine
NGC	Neuroglycan C
NGPF1	Neurite growth-promoting factor 1
NT-3	Neurotrophin-3
NT	Neurotrophins
P	Postnatal day
PLL	Poly-L-lysine
PTN	Pleiotrophin
RPTPβ/ζ	Receptor protein tyrosine phosphatase β/ζ
SDC	Syndecan
SG	Spiral ganglion

Electronic supplementary material The online version of this article (https://doi.org/10.1007/s00221-019-05644-6) contains supplementary material, which is available to authorized users.

✉ Stefan Volkenstein
Stefan.Volkenstein@rub.de

[1] Department of Otorhinolaryngology, Head and Neck Surgery, St. Elisabeth-Hospital, Ruhr-University Bochum, Bleichstr. 15, 44787 Bochum, Germany

[2] Department of Cell Morphology and Molecular Neurobiology, Faculty of Biology and Biotechnology, Ruhr-University Bochum, Universitätsstr. 150, 44801 Bochum, Germany

SGN Spiral ganglion neuron
SMN Spinal motor neuron

Introduction

In mammals, auditory information is received by hair cells within the sensory epithelium of the cochlea and transduced via different subtypes of spiral ganglion (SG) neurons (SGNs) to the brain (Nayagam et al. 2011; Zhang and Coate 2017). A variety of reasons like aging, acoustic trauma, genetic defects or ototoxic drugs may cause sensorineural hearing loss (Furness 2015). An irreversible damage to cochlear hair cells (HCs) is, therefore, often followed by a degeneration of SGNs (Dodson and Mohuiddin 2000).

When hearing aids do not originate satisfying speech discrimination, cochlear implants (CIs) are the only available therapeutic option for these patients with severe to profound sensorineural hearing loss. CIs replace HC functions in the auditory pathway. Until now, more than 600,000 patients worldwide received CIs (Nguyen et al. 2017). CIs bypass the HC function by converting sound information to a pulsatile electrical stimulation to the SGNs (Eshraghi et al. 2012; Geleoc and Holt 2014). CIs promote the survival of SGNs by electrical stimulation (Leake et al. 1999). More sophisticated strategies aim at an improved survival of SGNs by simultaneous electrical stimulation provided by the CI and supplementary treatment with neurotrophins (NTs) (Budenz et al. 2012). Neurotrophin-3 (NT-3) overexpressed by gene therapy in combination with a CI enhanced the SGN density in an animal model in vivo (Pfingst et al. 2017). So far, a positive impact on SGN survival or peripheral auditory fiber regrowth has been reported for several NTs, e.g., brain-derived neurotrophic factor (BNDF), NT-3, bone morphogenetic protein-2 (BMP-2), glial cell line-derived neurotrophic factor (GDNF) and leukemia inhibitory factor (LIF) (Bodmer et al. 2002; Euteneuer et al. 2013; Gillespie et al. 2001; Miller et al. 1997; Volkenstein et al. 2009).

An interesting novel candidate in the context of neuroprotection and neurite outgrowth of SGNs is pleiotrophin (PTN). It is a 17-kDa protein that belongs to the heparin-binding midkine (MK) family and shares a high homology (> 50%) with MK (Milner et al. 1989). PTN is also known as heparin-binding brain mitogen (HBBM), heparin-binding growth factor 8 (HBGF-8), neurite growth-promoting factor 1 (NGPF1), heparin affinity regulatory peptide (HARP) and heparin-binding growth-associated molecule (HB-GAM). PTN has a plethora of effects on different cell types, as indicated by its name (Kadomatsu et al. 2013). For example, PTN protects spinal motor neurons (SMN) against chronic excitotoxic injury and initiates an increasing outgrowth of motor axons, and is consequently a neurotrophic factor for SMNs (Mi et al. 2007). PTN also stimulates neurite outgrowth in perinatal rat brain neurons (Rauvala 1989; Rauvala et al. 1994). Knockout mice lacking PTN and MK exhibit severe deficits in auditory brainstem responses (Sone et al. 2011). PTN shows a wide expression pattern. First isolated from bovine uterus (Milner et al. 1989), it is also expressed in the central and peripheral nervous system, including the cochlea of mice up to one week after birth (Zou et al. 2006). Various receptors mediate PTN signaling, including anaplastic lymphoma kinase (ALK), α_v integrin, β_3 integrin, receptor protein tyrosine phosphatase (RPTP) β/ζ, neuroglycan C (NGC), low-density lipoprotein receptor-related protein (LRP) 1 and syndecan (SDC) 3 (Xu et al. 2014). Taken together, PTN is a promising candidate for new studies regarding neuroprotection and neurite outgrowth of SGNs.

In the present study, we investigated for the first time whether PTN has a neurotrophic effect and tested its influence on neurite outgrowth of SGNs in organotypic SG explants as well as of dissociated SGNs. Whereas SG explants allow to investigate cells in a complex cellular environment, dissociated SGNs receive reduced influence from surrounding cells and have direct contact to the PTN-containing medium.

Pleiotrophin significantly increased the number and neurite length of dissociated SGNs. To address the question which receptors mediate the observed effects of PTN, the expression of different potential PTN-related receptors in the mouse SG was investigated.

General methods

Animals

Postnatal day 4 (P4) BALB/c mice (Charles River Laboratories, Sulzfeld, Germany) of both sexes were used for this study. This inbred strain displays normal hearing, also in aged animals (Zheng et al. 1999). All animals were handled according to the German animal protection law. Experiments were approved by the animal care committee of North Rhine-Westphalia, Germany, based at the LANUV (Landesamt für Natur, Umwelt und Verbraucherschutz). Mice had continuous free access to chow and water, and were housed in the animal facility of the Ruhr-University Bochum (Faculty of Medicine) under a twelve-hour light–dark cycle and pathogen-free conditions.

SG dissection and cultivation of organotypic SG explants and dissociated SGNs

Postnatal mice were decapitated using a surgical scissor, according to the local guidelines for the experimental use

of animals. The SG was dissected as described previously (Kwiatkowska et al. 2016; Volkenstein et al. 2009, 2012).

After decapitation, the skin was removed from the skull and the skull was opened midsagittally. The brain was removed and the temporal bones were cut in midline and transferred into a Petri dish (35 × 10 mm; BD Falcon, New York, USA) with ice cold Dulbecco`s phosphate-buffered saline (DPBS; Gibco, Waltham, Massachusetts, USA). After removal of the bony capsule, the membranous cochlea was peeled off and the SG was separated from the modiolus. Afterwards, the stria vascularis and the layer of hair cells were dissected. For the organotypic cell culture, the SG was cut into 4–6 equal parts of 400–500 µm in diameter. For the dissociated cell culture, 8 complete cochleae were placed in 270 µl DPBS. Then, 30 µl Dispase (50 units/ml) was added and incubated for 40 min at 37 °C. Subsequently, the cochleae were placed in 500 µl DPBS and incubated for 40 min at room temperature (RT). After this, only the cochleae were transferred into an empty 2000-µl centrifuge tube. The dissociation was performed by pipetting up and down. Cells were transferred in 1400 µl basic medium (BM) containing serum-free Dulbecco`s modified Eagle Medium/F12 (mixed 1:1) with 1× L-Glutamine (Gibco), 20 µl/ml B-27 Supplement (50×, Gibco), 10 µl/ml N-2 Supplement (100×, Gibco) and 50 mg/ml Ampicillin (Carl Roth, Karlsruhe, Germany) (Volkenstein et al. 2012).

For the cultivation of organotypic SG explants and dissociated SGNs, four-well culture dishes (Greiner Bio One, Kremsmünster, Austria) and eight-chamber culture slides (BD Biosciences, Fraklin Lakes, New Jersey, USA) were coated with 100 µg/ml poly-L-Lysine (PLL; Sigma-Aldrich, St. Louis, Missouri, USA) in H_2O for 1 h at 37 °C. After washing twice with H_2O, dishes were coated with 10 µg/ml Laminin (LN; Sigma-Aldrich) in DPBS for 1 h at 37 °C. Prior to SG explant or SGN transfer, the wells were rinsed twice with DPBS and covered with culture medium until the final conditions were applied.

Explants were cultured in a four-well culture dish in BM under different conditions: BM in a serial dilution with PTN (PTN+; in every condition from 1:4 to 1:16) supplemented with 10 ng/ml BDNF (brain-derived neurotrophic factor; Invitrogen) and 20 ng/ml NT-3 (Sigma-Aldrich), BM in a serial dilution without PTN (PTN−; in every condition from 1:4 to 1:16) supplemented with 10 ng/ml BDNF (Invitrogen) and 20 ng/ml NT-3 (Sigma-Aldrich). Each coated culture well was filled with 50 µl culture medium as described above. Afterwards, the explants were placed in the middle of each culture well and incubated for 3 days at 37 °C with 5% CO_2 (FORMA Series II, Thermo Scientific, Waltham, Massachusetts, USA). After 24 h, 20 µl culture medium with equal condition was added.

Dissociated cells were seeded in wells of eight-chamber culture slides (BD Biosciences) in a density of 1.25×10^5 cells/300 µl. The cell suspensions were incubated for 3 days at 37 °C with 5% CO_2 (FORMA Series II, Thermo Scientific) under the same conditions as described for the explant culture system. As the same medium was used for the dissociated and explant culture, both culture conditions include supportive cells, e.g., glia cells.

PTN overexpression

For PTN overexpression, HEK293T cells (established by the group around M. P. Calos; DuBridge et al. 1987) were cultivated in medium containing DMEM, supplemented with 10% (v/v) fetal calf serum, 100 µg/ml Penicillin/Streptomycin and 1% (v/v) HEPES at 37 °C and 6% CO_2. For cell transfection, 100 µl of 2.5 M $CaCl_2$ was mixed with 20 µg plasmid DNA (full-length rat PTN in pcDNA™3.1/myc-His (Mi et al. 2007). The volume was filled up with H_2O to a total volume of 1 ml, before 1 ml of 2 x HBS (280 mM NaCl, 10 mM KCl, 1,5 mM $Na_2HPO_4 \times 2\ H_2O$, 12 mM dextrose, 50 mM HEPES, pH 7.05) was added dropwise to cells in a 10-cm culture dish. Subsequently, cells were incubated for 5 h at 37 °C and 6% CO_2, and then washed with PBS and cultivated in fresh medium for 65 h until the conditioned medium with overexpressed PTN was collected. For the PTN-negative control condition, medium from non-transfected HEK293T cells was also collected after 65 h. The concentration of PTN has previously been described between 80 and 100 ng/ml (Mi et al. 2007), resulting in 20–25 ng/ml for the 1:4, 10–12.5 ng/ml for the 1:8 and 5–6.25 ng/ml for the 1:16 condition.

Immunocytochemistry

Immunocytochemical stainings were performed as described previously (Kwiatkowska et al. 2016). In brief, after cultivation for 3 days, SG cells and explants were fixed in 4% Paraformaldehyde (SAFC, Biosciences, St. Louis, Missouri, USA) for 5 min. All steps were performed at RT unless specified otherwise. SG cells and explants were rinsed twice with DPBS and permeabilized with PBT-1 (PBS containing 0.1% Triton X-100; Sigma-Aldrich) and 1% bovine serum albumin (BSA; PAN Biotech, Aidenbach, Germany) for 30 min. To visualize SGN neurites, cultures were stained with anti-NF-200 antibody (anti-Neurofilament-200; mouse monoclonal IgG1, 1:500, Linaris, Dossenheim, Germany) in PBT-1 at 4 °C overnight. The primary antibody solution was rinsed twice with PBT-1 for 5 min before SG cells and explants were washed for 5 min with PBT-2 (0.1% Triton X-100 and 0.1% BSA in PBS). Afterwards, SG cells and explants were incubated for 2 h using a FITC-conjugated secondary antibody (goat anti-mouse IgG, Jackson Immuno Research, West Grove, Pennsylvania, USA) diluted 1:100 in PBT-2. SG cells and explants were rinsed twice with

PBT-2 for 5 min and cell nuclei were stained with DAPI (4,6-diamidino-2-phenylindole; 1:5000 in PBS; Invitrogen) for 15 min. Cells and explants were washed twice with PBS for 5 min and mounted in ImmunoSelect medium (Jackson Immuno Research).

Analysis of organotypic SG explants and dissociated SGNs

All analyses were performed with an inverted microscope (BX40, Olympus). To analyze organotypic explants, the number of neurites and neurite length were measured. Explants were photographed with a digital camera (DP50, Olympus) and each neurite was traced from the edge of the explant to its termination. Convoluted neurites were not being measured. The total number of neurites per explant was counted from all measured neurites.

Total number of neurons, neuronal morphology and the neurite length of the dissociated SGNs were analyzed. To assess the total cell number, all adherent cells with an unambiguous cell nucleus were counted, without regard to the morphology or the number of processes. Large cell aggregates were excluded.

The neuronal morphology was identified according to Whitlon et al. (2007). SGN morphology was evaluated from at least 5 random fields of view per well. The percentage for each neuron type was calculated from the total number of neurons.

For the neurite length measurements, pictures were taken from five fields of view with a digital camera (DP50, Olympus), according to Whitlon et al. (2007). The longest neurite in each field of view was measured. In case that 5 or less neurons were present in a well, the neurites of all neurons were measured. All analyses were performed with an image analysis program (ImageJ 1.49v, plug-in NeuronJ Version 1.4.3) (Meijering et al. 2004).

RNA isolation, cDNA synthesis and reverse-transcription polymerase chain reaction (RT-PCR)

SG tissue of 3 mice was isolated as described above, pooled and frozen on dry ice. Total RNA was isolated and purified according to the manufacturer's instructions using the ReliaPrep™ RNA Tissue Miniprep System kit (Promega, Madison, USA). RNA concentration and purity were assessed by spectrophotometry (BioSpectrometer, Eppendorf, Hamburg, Germany). To obtain cDNA, 1 µg RNA was reverse-transcribed using the First Strand cDNA Synthesis kit with random hexamer primers (Thermo Fisher Scientific, Waltham, MA, USA). RT-PCR was performed with 1 µl cDNA using Taq DNA Polymerase (Sigma-Aldrich) in a Mastercycler Gradient (Eppendorf, Hamburg, Germany) using various primers (Supplemental Tab. 1) at the following conditions: 94 °C for 5 min (initial denaturation), 36 cycles of 94 °C for 30 s (denaturation), 60 °C for 35 s (annealing) and 72 °C for 1 min (elongation), followed by 72 °C for 5 min (final elongation). The samples were documented after agarose gel electrophoresis under UV light. The identity of the amplicons was confirmed by the sequencing service of the Ruhr-University Bochum. Sequences were analyzed with Sequence Scanner software (Applied Biosystems, Carlsbad, USA) and the BLAST tool of the National Center for Biotechnology Information database (NCBI; Bethesda, USA).

Western blot

SGs of 4 mice were isolated, pooled and homogenized in 60 µl lysis buffer (60 mM *n*-octyl-ß-D-glucopyranoside, 50 mM sodium acetate, 50 mM Tris chloride pH 8.0 and 2 M urea) containing a protease inhibitor cocktail (1:10; Sigma-Aldrich) on ice for 2 h. The protein lysate was centrifuged at 14,000×*g* at 4 °C for 30 min. Protein concentration of the supernatant was determined with a BCA Protein Assay kit (Pierce, Thermo Fisher Scientific, Rockford, Illinois, USA). Afterwards, 4× sodium dodecyl sulfate (SDS) sample buffer was added to the protein sample (20 µg). The protein sample was denaturized at 95 °C for 5 min and separated via SDS polyacrylamide gel electrophoresis (SDS-PAGE) using a 4–10% polyacrylamide gradient gels. After separation, proteins were transferred to polyvinylidene difluoride (PVDF) membranes (Roth, Karlsruhe, Germany) by Western blotting. Membranes were incubated in blocking solution containing 5% w/v milk powder in Tris-buffered saline (TBS) and Tween 20 (TBST) at RT for 1 h. Primary antibodies diluted in blocking solution were used against Lrp1 (85 kDa, rabbit, 1:10,000; ab92544, Abcam, Berlin, Germany), RPTPβ/ζ-isoforms (KAF13 antibody; > 150 kDa, rabbit, 1:5000) (Faissner et al. 1994), the DSD-1 epitope (473HD antibody; > 150 kDa, rat, 1:100) (Clement et al. 1998) and α-tubulin (clone DM1A; 50 kDa, mouse, 1:10,000; Sigma-Aldrich). After incubation over night at 4 °C, membranes were washed in TBST, before horseradish peroxidase (HRP)-coupled secondary antibodies (Dianova) were diluted 1:5000 in blocking solution and applied. After incubation at RT for 1 h, membranes were washed in TBST and finally in TBS. To detect proteins, ECL Substrate solutions (Bio-Rad Laboratories GmbH, Munich, Germany) were mixed 1:1, added to the membranes and incubated at RT for 5 min. Immunoreactivity of proteins was detected with a MicroChemi Chemiluminescence Reader (Biostep, Burkhardtsdorf, Germany).

Statistical evaluation

Statistical analysis was performed with GraphPad Prism (Version 6.01, GraphPad Software, La Jolla California USA). For the statistical analysis of neuronal viability, the number of neurites and the neurite length, one-way ANOVA followed by Bonferroni multiple comparisons test was performed. Data were expressed as mean ± standard error of mean (SEM). The Chi-square test was used to analyze neuronal morphology. Values of $p < 0.05$ were considered statistically significant.

Image processing

Brightness and contrast of images were adjusted using Adobe Photoshop and artwork was created with Adobe Illustrator (both version CS6, Adobe Inc., San José California USA).

Results

Influence of PTN on neurite number and neurite length in SG explants

To analyze a potential effect of PTN on neurite outgrowth of SGNs in vitro, SGNs were cultivated as organotypic explants without and in the presence of PTN using decreasing dilutions of PTN-conditioned medium (1:4, 1:8 and 1:16). After 3 days, explants were immunostained against neurofilament-200 (NF-200; Fig. 1a, b). Quantification revealed a comparable number of neurites per explant ($p > 0.999$ for all dilutions) without and after PTN treatment (Table 1; Fig. 1c). A slight, non-significant increase in the neurite length of SGNs was measured in the presence of PTN (1:4, $p = 0.178$; 1:8, $p = 0.159$; 1:16, $p > 0.999$; Table 2; Fig. 1d).

Influence of PTN on neurite length, cell number and morphology of dissociated SGNs

Dissociated SGNs were cultivated in vitro for 3 days, either without PTN (PTN−) or in the presence of PTN (PTN+; Fig. 2a, b). Analysis of NF-200-immunostained SGNs showed a significantly increased neurite length after cultivation with PTN 1:4 (PTN+: 1023.00 ± 74.07 µm; PTN−: 221.30 ± 20.19 µm; $p = 0.001$; Table 3; Fig. 2c). No significant difference was found for lower PTN levels (1:8, $p = 0.258$; 1:16, $p = 0.399$). SGN numbers were significantly increased in the presence of PTN 1:4, indicating a promoting effect on the cell density in our dissociated SGN culture system (PTN+: 66.33 ± 6.96; PTN−: 19.67 ± 8.09; $p = 0.044$; Table 4; Fig. 2d). Cell morphological analysis revealed a comparable ratio of SGNs without neurites and with mono-, bi-, pseudouni- and multipolar morphology under all conditions (Table 5; Fig. 2e, f). Most of the SGNs displayed a monopolar morphology, followed by cells with a bipolar morphology. Only few pseudounipolar or multipolar cells were observed.

PTN-associated receptors in the SG

The expression of *Anaplastic lymphoma kinase* (*Alk*), α_v *Integrin (Itgav)*, β_3 *Integrin (Itgb3)*, *Receptor protein tyrosine phosphatase β/ζ* (*Ptprz1*), *Neuroglycan C* (*Ngc*), *Low density lipoprotein receptor-related protein 1* (*Lrp1*), *Syndecan 3* (*Sdc3*) and the housekeeping gene *β-Actin* (*Actb*) in the SG at postnatal day 4 (P4) was confirmed on mRNA level by RT-PCR (Fig. 3a). Furthermore, we confirmed the expression of LRP1 and RPTPβ/ζ, two important PTN receptors, on protein level in the SG (Fig. 3b). Finally, we were able to detect the DSD-1 carbohydrate epitope, a modification specifically found on RPTPβ/ζ.

Discussion

The present study was designed to analyze the influence of PTN on SGNs using an organotypic explant and dissociated cell culture system. Our data demonstrate that PTN has a beneficial effect on neurite length and the number of dissociated SGNs in vitro. However, only a moderate, statistically not significant effect on the neurite length was observed in the SG explants. Therefore, the results show the advantages and disadvantages of the different cell culture models, depending on the research question.

PTN has only a minor effect on SGN neurites in organotypic explants

No statistically significant difference in the number and length of neurites was found after PTN treatment in our organotypic SG explant model. Nevertheless, a tendency of an increased neurite length was observed. These findings are in line with other studies, which show that PTN increases the neurite number of primary cortical neurons in an in vitro oxygen and glucose deprivation model (Wang et al. 2014). PTN also enhanced the neurite length of SMNs cultivated as explants or as dissociated cells and of dorsal root ganglion (DRG) cultures (Mi et al. 2007). In their study, PTN improved the number of axons crossing the gray–white matter junction of SMNs.

The lack of statistically significant effects might be related to the explant model, in which the SGNs are in close contact to other cells, e.g., Schwann and hair cells (Hansen et al. 2001a, b). Those cell types are a source of additional signals including neurotrophic factors that influence the SGNs, which may cover potential effects of the PTN treatment. Therefore,

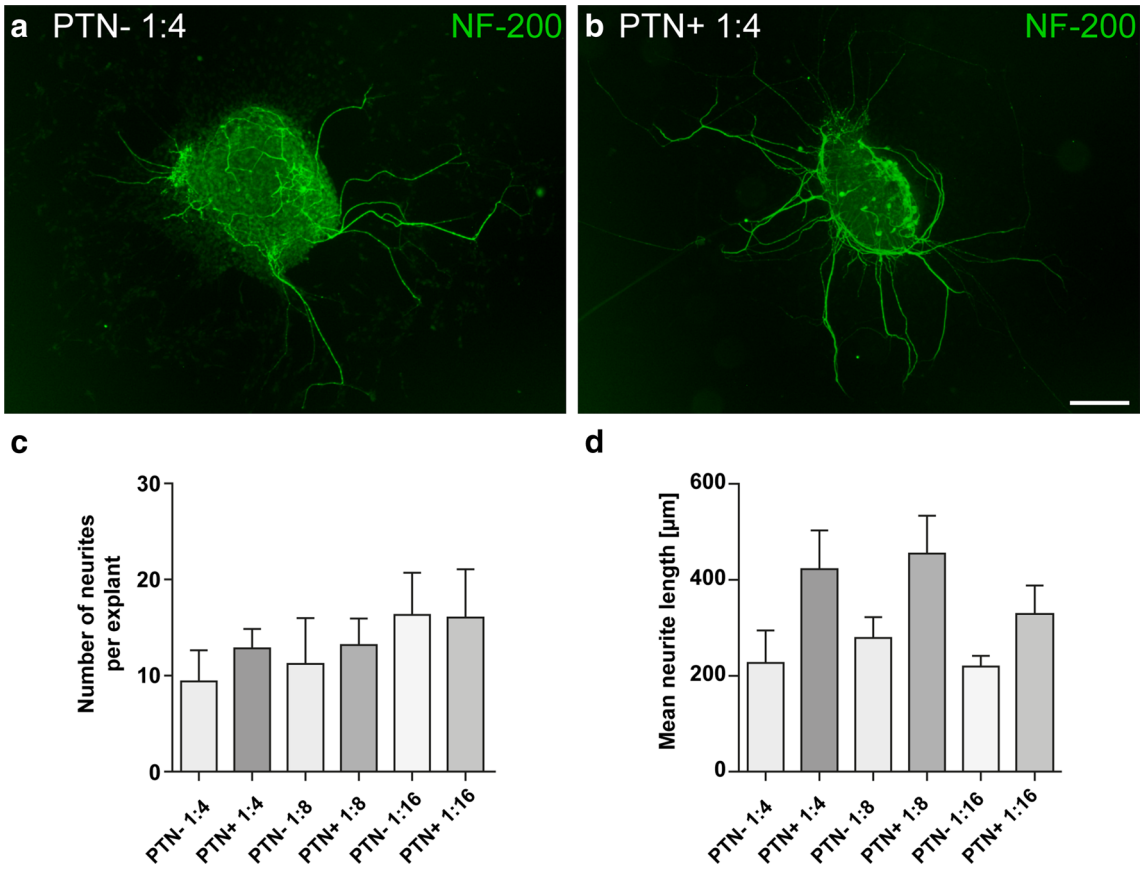

Fig. 1 The influence of PTN on the neurite number and neurite length of SG explants in vitro. **a**, **b** Representative fluorescence images display NF-200-immunostained SG explants after cultivation without PTN (PTN−; 1:4) and in the presence of PTN (PTN+; 1:4). **c** A comparable number of neurites per explant was observed following different treatments. **d** The mean neurite length of SGNs was quantified without and after PTN treatment (1:4, 1:8 and 1:16). The mean neurite length was comparable under all conditions. Data are shown as mean ± standard error of mean (SEM). Statistical analyses were performed using one-way ANOVA followed by Bonferroni multiple comparisons test. Scale bar = 100 µm

Table 1 Number of neurites per explant

Condition	Dilution	Mean	SEM	*p* value
PTN−	1:4	9.60	3.20	> 0.999
PTN+		12.80	2.04	
PTN−	1:8	11.17	4.81	> 0.999
PTN+		13.14	2.79	
PTN−	1:16	16.50	4.41	> 0.999
PTN+		16.00	5.07	

Data are shown as mean ± standard error of mean (SEM, $n = 4–7$). Statistical analyses were performed using one-way ANOVA followed by Bonferroni multiple comparisons test

Table 2 Mean neurite length of explants

Condition	Dilution	Mean	SEM	*p* value
PTN−	1:4	226.90	67.42	0.178
PTN+		421.70	81.25	
PTN−	1:8	279.00	43.26	0.159
PTN+		454.60	79.06	
PTN−	1:16	219.00	22.17	>0.999
PTN+		329.30	58.68	

Data are shown as mean ± standard error of mean (SEM, $n = 4–7$). Statistical analyses were performed using one-way ANOVA followed by Bonferroni multiple comparisons test

we analyzed the neurite length of SGNs using the dissociated SG culture model, where the cells are directly exposed to the PTN-containing medium and the distance between SGNs and neighboring cells is larger.

PTN increases the neurite length and number of dissociated SGNs in vitro

Dissociated SGNs showed a significantly increased neurite length and neuron number after PTN treatment. In this

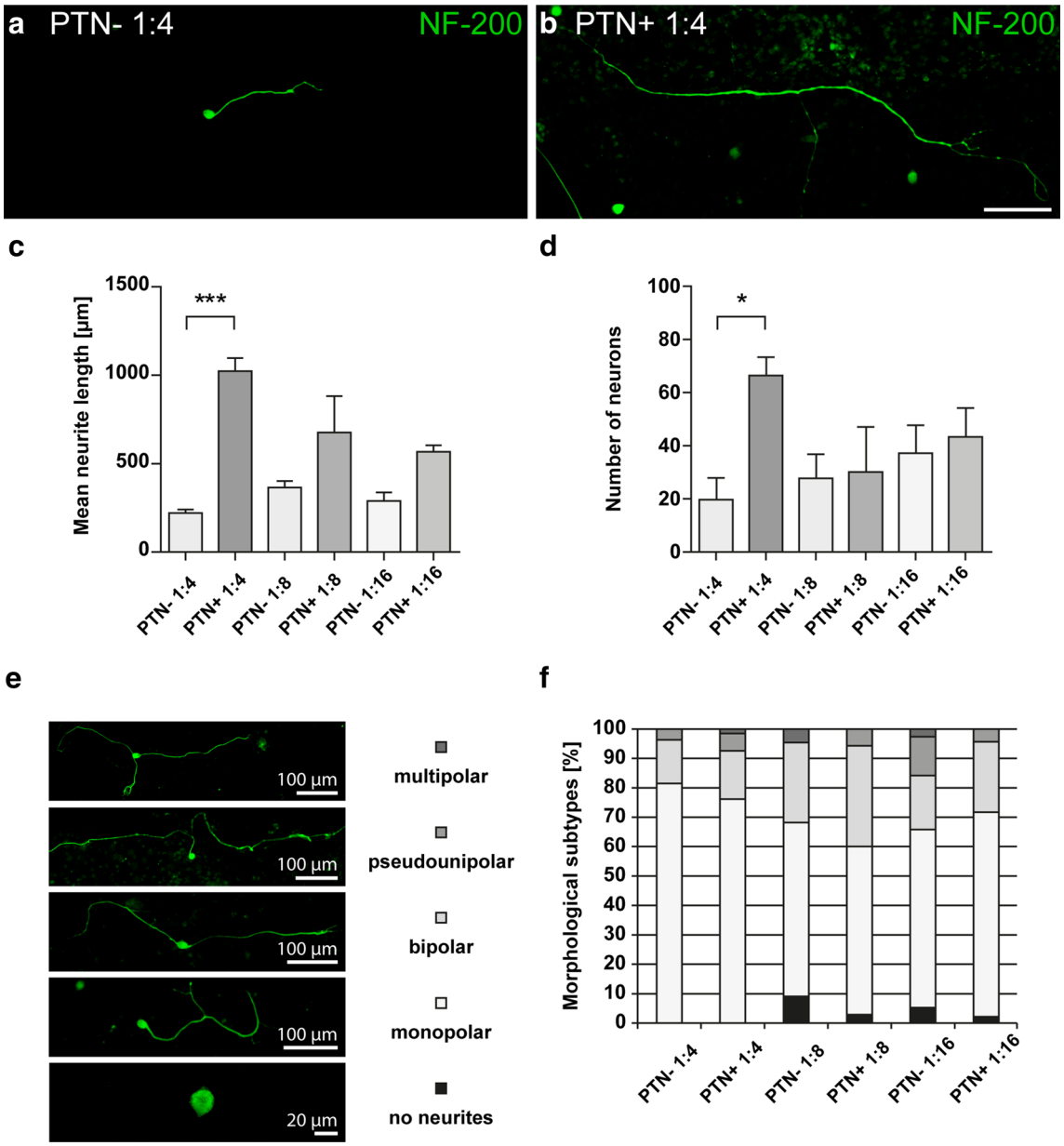

Fig. 2 The influence of PTN on the neurite length, adhesion, viability and morphology of SGNs in vitro. **a**, **b** Representative fluorescence images display NF-200-immunostained dissociated SGNs after cultivation without PTN (PTN−; 1:4) and in the presence of PTN (PTN+; 1:4). **c** After cultivation with PTN 1:4, a significantly increased neurite length of SGNs was observed. **d** To analyze SGN adhesion and viability, SGN numbers were quantified without and after PTN treatment (1:4, 1:8 and 1:16). SGN numbers were significantly increased in the presence of PTN, indicating a promoting effect on adhesion or viability of SGNs. **e**, **f** To analyze potential morphological changes, polarity of SGN neurites was monitored. The ratio of SGNs without neurites and with mono-, bi-, pseudouni- and multipolar morphology was comparable under all conditions. Data are shown as mean ± standard error of mean (SEM; **c**, **d**) or mean (**f**). Statistical analyses were performed using one-way ANOVA followed by Bonferroni multiple comparisons test. The comparison of the neuronal morphology was performed with the Chi-square test. $*p < 0.05$; $***p < 0.001$. Scale bar = 100 µm

regard, potential pathways involved in the mediation of PTN-induced effects are of great interest.

Recent in vivo and in vitro experiments revealed a trophic effect of PTN on the survival of dopaminergic neurons (Hida et al. 2003, 2007). PTN had also a positive effect on the survival of DRG neurons co-cultured with PTN-secreting pancreatic cancer cells (Yao et al. 2011, 2014). In contrast, another study on dissociated SMN and DRG cultures demonstrated just an enhancement of the neurite length, but no increase in the cell number following PTN treatment (Mi

Table 3 Mean neurite length of dissociated cells

Condition	Dilution	Mean	SEM	*p* value
PTN−	1:4	221.30	20.19	0.001
PTN+		1023.00	74.07	
PTN−	1:8	365.20	36.43	0.258
PTN+		676.20	205.50	
PTN−	1:16	290.00	47.36	0.399
PTN+		563.50	39.71	

Data are shown as mean ± standard error of mean (SEM, $n = 3$). Statistical analyses were performed using one-way ANOVA followed by Bonferroni multiple comparisons test

Table 4 Number of neurons

Condition	Dilution	Mean	SEM	*p* value
PTN−	1:4	19.67	8.09	0.044
PTN+		66.33	6.96	
PTN−	1:8	27.33	9.06	>0.999
PTN+		30.00	17.04	
PTN−	1:16	37.33	10.48	>0.999
PTN+		43.33	10.91	

Data are shown as mean ± standard error of mean (SEM, $n = 3$). Statistical analyses were performed using one-way ANOVA followed by Bonferroni multiple comparisons test

et al. 2007). This shows that PTN affects neurons in a cell-type and context-specific manner.

Morphology of dissociated SGNs

Comparison of the cell morphologies showed that monopolar and bipolar neurons were the most frequent subtypes. A previous study had shown that the growth factors NT-3, BDNF, LIF and especially combinations of those factors enhance the proportion of bipolar neurons and reduce the number of neurons without neurites (Jin et al. 2013). However, in our culture conditions, PTN had no additional influence on neuronal morphology, as indicated by a similar distribution of neuronal subtypes compared to other neurotrophic factors. It is feasible that the combination of different factors, including PTN, might have an effect on SGN morphology.

Potential pathways underlying PTN signaling in the SG

To identify potential underlying signaling pathways of PTN in the mouse SG, we performed RT-PCR analyses for several receptor molecules. Anaplastic lymphoma kinase (ALK), integrin $\alpha_v\beta_3$, receptor protein tyrosine phosphatase β/ζ (RPTPβ/ζ), neuroglycan C (NGC), low-density lipoprotein

Table 5 Neuron morphology distribution

Condition	Dilution	Monopolar	Bipolar	Pseudo-unipolar	Multipolar	No neurites
PTN−	1:4	81.48	14.81	3.71	0	0
PTN+		76.12	16.42	5.97	1.49	0
PTN−	1:8	59.09	27.28	0	4.55	9.08
PTN+		57.14	34.29	5.71	0	2.86
PTN−	1:16	60.53	18.42	13.16	2.63	5.26
PTN+		69.57	23.91	4.35	0	2.17

Data are shown as mean. The comparison of the neuronal morphology was performed with the Chi-square test

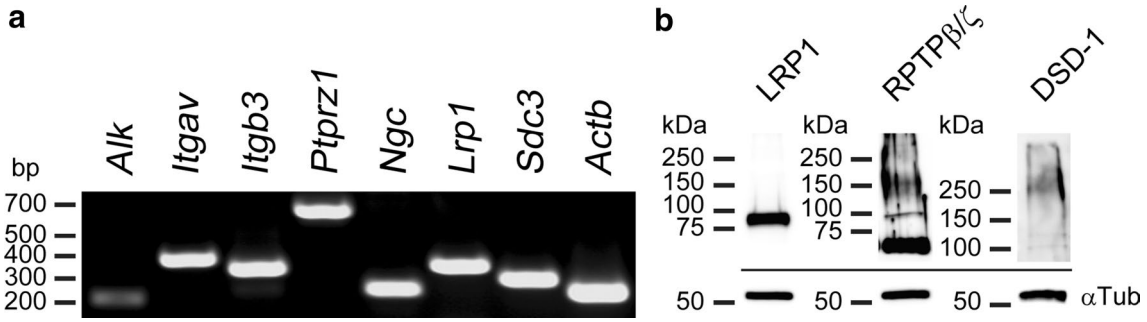

Fig. 3 Expression of PTN-associated receptors in the mouse SG at postnatal day 4. **a** The expression of *Alk*, *Itgav*, *Itgb3*, *Ptprz1*, *Ngc*, *Lrp1*, *Sdc3* and the housekeeping gene *Actb* in the SG was confirmed on mRNA level by RT-PCR. **b** LRP1 and RPTPβ/ζ protein levels as well as the DSD-1 carbohydrate epitope, a modification of RPTPβ/ζ, were detected via Western blot. α-tubulin (αTub) served as loading control. *bp* base pairs, *kDa* kilo Dalton

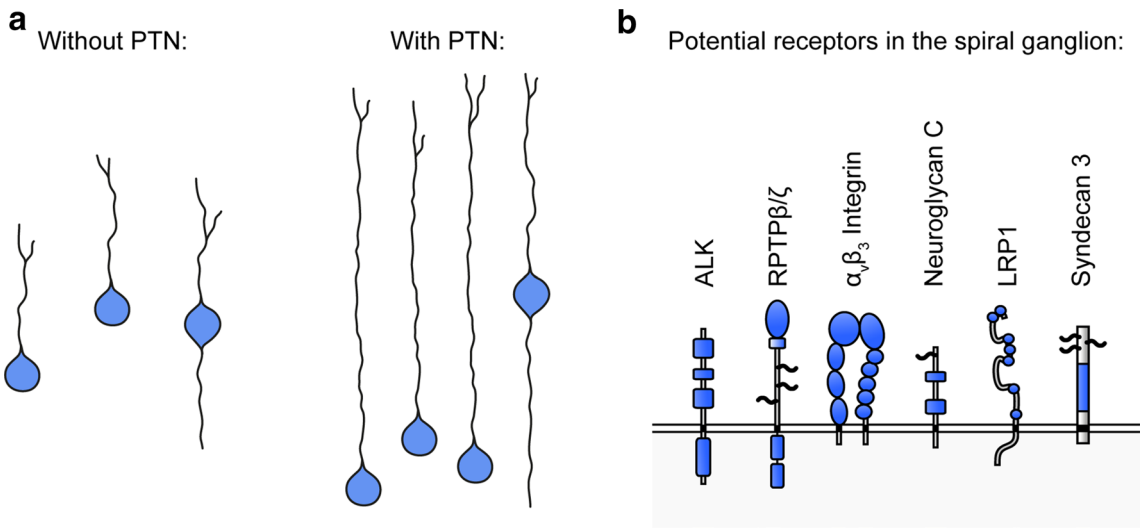

Fig. 4 Cartoon illustrating the influence of PTN on SGNs in vitro and expression of PTN-related receptors. **a** Morphology of SGNs in the absence and presence of PTN in vitro. An enhanced neurite length was observed after PTN treatment, while polarity of neurons was comparable under both conditions. **b** Expression of potential PTN receptors in the SG

receptor related protein (LRP) and syndecan 3 (SDC3) have been reported as PTN-associated receptors in various tissues (Xu et al. 2014). We could demonstrate that these receptors were expressed on mRNA level in the postnatal SG. Additionally, we were able to confirm the presence of LRP1 and RPTPβ/ζ proteins at this developmental stage, which points to the reliability of our mRNA analyses.

PTN mediates neurotrophic properties in SMN via the ALK pathway (Mi et al. 2007). Although expression of ALK has not been described previously, we identified its transcript in the postnatal SG.

Integrin $\alpha_v\beta_3$ induces endothelial cell migration through RPTPβ/ζ (Mikelis et al. 2009) and was found in the SGN. Kistrin, a potent inhibitor of $\alpha_v\beta_3$ integrin, reduced the mean neurite length of SG explants cultured on the extracellular matrix substrate LN (Aletsee et al. 2001). According to these findings, PTN might act through the $\alpha_v\beta_3$ integrin pathway on SGN neurite growth.

RPTPβ/ζ has important functions in the developing nervous system and displays mitogenic and neurite outgrowing activity (Asai et al. 2009; Maeda and Noda 1998). As shown by our expression analyses and previous reports, it is expressed in hair cells and SGNs (Kowalik and Hudspeth 2011; Kwiatkowska et al. 2016).

NGC is a brain-specific chondroitin sulfate proteoglycan that has neurite outgrowth-promoting effects on cortical neurons (Nakanishi et al. 2006). Also, process elongation of oligodendrocyte precursors is mediated by NGC (Ichihara-Tanaka et al. 2006).

LRP1 is a large transmembrane receptor with multiple functions in various processes, including lipoprotein metabolism, axon guidance and is a crucial neurotrophic factor for sensory neurons (Lillis et al. 2008; Yamauchi et al. 2013). Midkine-induced neuroprotection is transmitted via LRP (Muramatsu et al. 2000).

SDCs are a family of transmembrane heparan sulfate proteoglycans (Afratis et al. 2017). Previous studies suggest that PTN displays neurite outgrowth-promoting effects on cerebral neurons by binding to SDC3 (Raulo et al. 1994). Very recently, another heparan sulfate proteoglycan, glypican-2, was identified as a mediator of PTN-induced neurite outgrowth (Paveliev et al. 2016).

Conclusion

We could demonstrate that PTN has a promoting effect on neurite outgrowth and the number of dissociated SGNs in vitro. This effect was weaker in the explant culture. In addition, we identified PTN-associated receptors that are expressed in the postnatal SG, which potentially mediate the observed effects of PTN (Fig. 4). Further in vivo experiments with simultaneous electrical stimulation and supplementary treatment with PTN should be performed.

Acknowledgements This study was supported by MED-EL Deutschland GmbH research grant PVBO2012/2. We gratefully acknowledge Susanne Kanabey and Sabine Kindermann for excellent technical assistance.

Compliance with ethical standards

Conflict of interest The authors declare that they have no conflict of interest.

References

Afratis NA, Nikitovic D, Multhaupt HA, Theocharis AD, Couchman JR, Karamanos NK (2017) Syndecans-key regulators of cell signaling and biological functions. FEBS J 284:27–41

Aletsee C, Mullen L, Kim D, Pak K, Brors D, Dazert S, Ryan AF (2001) The disintegrin kistrin inhibits neurite extension from spiral ganglion explants cultured on laminin. Audiol Neurootol 6:57–65

Asai H, Yokoyama S, Morita S, Maeda N, Miyata S (2009) Functional difference of receptor-type protein tyrosine phosphatase zeta/beta isoforms in neurogenesis of hippocampal neurons. Neuroscience 164:1020–1030

Bodmer D, Gloddek B, Ryan AF, Huverstuhl J, Brors D (2002) Inhibition of the c-Jun N-terminal kinase signaling pathway influences neurite outgrowth of spiral ganglion neurons in vitro. Laryngoscope 112:2057–2061

Budenz CL, Pfingst BE, Raphael Y (2012) The use of neurotrophin therapy in the inner ear to augment cochlear implantation outcomes. Anat Rec (Hoboken) 295:1896–1908

Clement AM, Nadanaka S, Masayama K, Mandl C, Sugahara K, Faissner A (1998) The DSD-1 carbohydrate epitope depends on sulfation, correlates with chondroitin sulfate D motifs, and is sufficient to promote neurite outgrowth. J Biol Chem 273:28444–28453

Dodson HC, Mohuiddin A (2000) Response of spiral ganglion neurones to cochlear hair cell destruction in the guinea pig. J Neurocytol 29:525–537

DuBridge RB, Tang P, Hsia HC, Leong PM, Miller JH, Calos MP (1987) Analysis of mutation in human cells by using an Epstein-Barr virus shuttle system. Mol Cell Biol 1:379–387

Eshraghi AA, Nazarian R, Telischi FF, Rajguru SM, Truy E, Gupta C (2012) The cochlear implant: historical aspects and future prospects. Anat Rec (Hoboken) 295:1967–1980

Euteneuer S, Yang KH, Chavez E, Leichtle A, Loers G, Olshansky A, Pak K, Schachner M et al (2013) Glial cell line-derived neurotrophic factor (GDNF) induces neuritogenesis in the cochlear spiral ganglion via neural cell adhesion molecule (NCAM). Mol Cell Neurosci 54:30–43

Faissner A, Clement A, Lochter A, Streit A, Mandl C, Schachner M (1994) Isolation of a neural chondroitin sulfate proteoglycan with neurite outgrowth promoting properties. J Cell Biol 126:783–799

Furness DN (2015) Molecular basis of hair cell loss. Cell Tissue Res 361:387–399

Geleoc GS, Holt JR (2014) Sound strategies for hearing restoration. Science 344:1241062

Gillespie LN, Clark GM, Bartlett PF, Marzella PL (2001) LIF is more potent than BDNF in promoting neurite outgrowth of mammalian auditory neurons in vitro. NeuroReport 12:275–279

Hansen MR, Vijapurkar U, Koland JG, Green SH (2001a) Reciprocal signaling between spiral ganglion neurons and Schwann cells involves neuregulin and neurotrophins. Hear Res 161:87–98

Hansen MR, Zha XM, Bok J, Green SH (2001b) Multiple distinct signal pathways, including an autocrine neurotrophic mechanism, contribute to the survival-promoting effect of depolarization on spiral ganglion neurons in vitro. J Neurosci 21:2256–2267

Hida H, Jung CG, Wu CZ, Kim HJ, Kodama Y, Masuda T, Nishino H (2003) Pleiotrophin exhibits a trophic effect on survival of dopaminergic neurons in vitro. Eur J Neurosci 17:2127–2134

Hida H, Masuda T, Sato T, Kim TS, Misumi S, Nishino H (2007) Pleiotrophin promotes functional recovery after neural transplantation in rats. NeuroReport 18:179–183

Ichihara-Tanaka K, Oohira A, Rumsby M, Muramatsu T (2006) Neuroglycan C is a novel midkine receptor involved in process elongation of oligodendroglial precursor-like cells. J Biol Chem 281:30857–30864

Jin Y, Kondo K, Ushio M, Kaga K, Ryan AF, Yamasoba T (2013) Developmental changes in the responsiveness of rat spiral ganglion neurons to neurotrophic factors in dissociated culture: differential responses for survival, neuritogenesis and neuronal morphology. Cell Tissue Res 351:15–27

Kadomatsu K, Kishida S, Tsubota S (2013) The heparin-binding growth factor midkine: the biological activities and candidate receptors. J Biochem 153:511–521

Kowalik L, Hudspeth AJ (2011) A search for factors specifying tonotopy implicates DNER in hair-cell development in the chick's cochlea. Dev Biol 354:221–231

Kwiatkowska M, Reinhard J, Roll L, Kraft N, Dazert S, Faissner A, Volkenstein S (2016) The expression pattern and inhibitory influence of Tenascin-C on the growth of spiral ganglion neurons suggest a regulatory role as boundary formation molecule in the postnatal mouse inner ear. Neuroscience 319:46–58

Leake PA, Hradek GT, Snyder RL (1999) Chronic electrical stimulation by a cochlear implant promotes survival of spiral ganglion neurons after neonatal deafness. J Comp Neurol 412:543–562

Lillis AP, Van Duyn LB, Murphy-Ullrich JE, Strickland DK (2008) LDL receptor-related protein 1: unique tissue-specific functions revealed by selective gene knockout studies. Physiol Rev 88:887–918

Maeda N, Noda M (1998) Involvement of receptor-like protein tyrosine phosphatase zeta/RPTPbeta and its ligand pleiotrophin/heparin-binding growth-associated molecule (HB-GAM) in neuronal migration. J Cell Biol 142:203–216

Meijering E, Jacob M, Sarria JC, Steiner P, Hirling H, Unser M (2004) Design and validation of a tool for neurite tracing and analysis in fluorescence microscopy images. Cytometry A 58:167–176

Mi R, Chen W, Hoke A (2007) Pleiotrophin is a neurotrophic factor for spinal motor neurons. Proc Natl Acad Sci USA 104:4664–4669

Mikelis C, Sfaelou E, Koutsioumpa M, Kieffer N, Papadimitriou E (2009) Integrin alpha(v)beta(3) is a pleiotrophin receptor required for pleiotrophin-induced endothelial cell migration through receptor protein tyrosine phosphatase beta/zeta. FASEB J 23:1459–1469

Miller JM, Chi DH, O'Keeffe LJ, Kruszka P, Raphael Y, Altschuler RA (1997) Neurotrophins can enhance spiral ganglion cell survival after inner hair cell loss. Int J Dev Neurosci 15:631–643

Milner PG, Li YS, Hoffman RM, Kodner CM, Siegel NR, Deuel TF (1989) A novel 17 kD heparin-binding growth factor (HBGF-8) in bovine uterus: purification and N-terminal amino acid sequence. Biochem Biophys Res Commun 165:1096–1103

Muramatsu H, Zou K, Sakaguchi N, Ikematsu S, Sakuma S, Muramatsu T (2000) LDL receptor-related protein as a component of the midkine receptor. Biochem Biophys Res Commun 270:936–941

Nakanishi K, Aono S, Hirano K, Kuroda Y, Ida M, Tokita Y, Matsui F, Oohira A (2006) Identification of neurite outgrowth-promoting domains of neuroglycan C, a brain-specific chondroitin sulfate proteoglycan, and involvement of phosphatidylinositol 3-kinase and protein kinase C signaling pathways in neuritogenesis. J Biol Chem 281:24970–24978

Nayagam BA, Muniak MA, Ryugo DK (2011) The spiral ganglion: connecting the peripheral and central auditory systems. Hear Res 278:2–20

Nguyen TAK, Cavuscens S, Ranieri M, Schwarz K, Guinand N, van de Berg R, van den Boogert T, Lucieer F et al (2017) Characterization of cochlear, vestibular and cochlear-vestibular electrically evoked compound action potentials in patients with a vestibulocochlear implant. Front Neurosci 11:645

Paveliev M, Fenrich KK, Kislin M, Kuja-Panula J, Kulesskiy E, Varjosalo M, Kajander T, Mugantseva E et al (2016) HB-GAM

(pleiotrophin) reverses inhibition of neural regeneration by the CNS extracellular matrix. Sci Rep 6:33916

Pfingst BE, Colesa DJ, Swiderski DL, Hughes AP, Strahl SB, Sinan M, Raphael Y (2017) neurotrophin gene therapy in deafened ears with cochlear implants: long-term effects on nerve survival and functional measures. J Assoc Res Otolaryngol 18:731–750

Raulo E, Chernousov MA, Carey DJ, Nolo R, Rauvala H (1994) Isolation of a neuronal cell surface receptor of heparin binding growth-associated molecule (HB-GAM). Identification as N-syndecan (syndecan-3). J Biol Chem 269:12999–13004

Rauvala H (1989) An 18-kd heparin-binding protein of developing brain that is distinct from fibroblast growth factors. EMBO J 8:2933–2941

Rauvala H, Vanhala A, Castren E, Nolo R, Raulo E, Merenmies J, Panula P (1994) Expression of HB-GAM (heparin-binding growth-associated molecules) in the pathways of developing axonal processes in vivo and neurite outgrowth in vitro induced by HB-GAM. Brain Res Dev Brain Res 79:157–176

Sone M, Muramatsu H, Muramatsu T, Nakashima T (2011) Morphological observation of the stria vascularis in midkine and pleiotrophin knockout mice. Auris Nasus Larynx 38:41–45

Volkenstein S, Brors D, Hansen S, Minovi A, Laub M, Jennissen HP, Dazert S, Neumann A (2009) Influence of bone morphogenetic protein-2 on spiral ganglion neurite growth in vitro. Eur Arch Otorhinolaryngol 266:1381–1389

Volkenstein S, Kirkwood JE, Lai E, Dazert S, Fuller GG, Heller S (2012) Oriented collagen as a potential cochlear implant electrode surface coating to achieve directed neurite outgrowth. Eur Arch Otorhinolaryngol 269:1111–1116

Wang Y, Qiu B, Liu J, Zhu WG, Zhu S (2014) Cocaine- and amphetamine-regulated transcript facilitates the neurite outgrowth in cortical neurons after oxygen and glucose deprivation through PTN-dependent pathway. Neuroscience 277:103–110

Whitlon DS, Grover M, Tristano J, Williams T, Coulson MT (2007) Culture conditions determine the prevalence of bipolar and monopolar neurons in cultures of dissociated spiral ganglion. Neuroscience 146:833–840

Xu C, Zhu S, Wu M, Han W, Yu Y (2014) Functional receptors and intracellular signal pathways of midkine (MK) and pleiotrophin (PTN). Biol Pharm Bull 37:511–520

Yamauchi K, Yamauchi T, Mantuano E, Murakami K, Henry K, Takahashi K, Campana WM (2013) Low-density lipoprotein receptor related protein-1 (LRP1)-dependent cell signaling promotes neurotrophic activity in embryonic sensory neurons. PLoS One 8:e75497

Yao J, Zhang M, Ma QY, Wang Z, Wang LC, Zhang D (2011) PAd-shRNA-PTN reduces pleiotrophin of pancreatic cancer cells and inhibits neurite outgrowth of DRG. World J Gastroenterol 17:2667–2673

Yao J, Li WY, Li SG, Feng XS, Gao SG (2014) Recombinant lentivirus targeting the pleotrophin gene reduces pleotrophin protein expression in pancreatic cancer cells and inhibits neurite outgrowth of dorsal root ganglion neurons. Mol Med Rep 9:999–1004

Zhang KD, Coate TM (2017) Recent advances in the development and function of type II spiral ganglion neurons in the mammalian inner ear. Semin Cell Dev Biol 65:80–87

Zheng QY, Johnson KR, Erway LC (1999) Assessment of hearing in 80 inbred strains of mice by ABR threshold analyses. Hear Res 130:94–107

Zou P, Muramatsu H, Sone M, Hayashi H, Nakashima T, Muramatsu T (2006) Mice doubly deficient in the midkine and pleiotrophin genes exhibit deficits in the expression of beta-tectorin gene and in auditory response. Lab Invest 86:645–653